IVYSPRING INTERNATIONAL PUBLISHER

Theranostics

2019; 9(2): 477-490. doi: 10.7150/thno.29361

Research Paper

Argon Mitigates Impaired Wound Healing Process and Enhances Wound Healing *In Vitro* and *In Vivo*

Jiaolin Ning[1,2*], Hailin Zhao[2*], Bin Chen[1*], Emma Zheling Mi[2*], Zhen Yang[1], Wenhan Qing[1], Kwok Wing Joyce Lam[2], Bin Yi[1], Qian Chen[1,2], Jianteng Gu[1✉], Thomas Ichim[3], Vladimir Bogin[3], Kaizhi Lu[1✉], Daqing Ma[2✉]

1. Department of Anesthesiology, Southwest Hospital, Third Military Medical University (Army Medical University), Chongqing, China
2. Anaesthetics, Pain Medicine and Intensive Care, Department of Surgery and Cancer, Faculty of Medicine, Imperial College London, Chelsea & Westminster Hospital, London, UK
3. Nobilis Therapeutics, Inc. 3042 NW Monte Vista Ter, Portland, OR 97210

*These authors contributed equally to this work.

✉ Corresponding authors: Daqing Ma, MD, PhD, FRCA, Anaesthetics, Pain Medicine and Intensive Care, Department of Surgery and Cancer, Faculty of Medicine, Imperial College London, Chelsea and Westminster Hospital, London, UK. Tel: (0044) 02033158495; Fax: (0044) 02033155109; E-mail: d.ma@imperial.ac.uk; Jianteng Gu (jiantenggu@hotmail.com) or Kaizhi Lu (lukaizhi2010@163.com).

Received: 2018.08.20; Accepted: 2018.10.04; Published: 2019.01.01

Abstract

Diabetic foot ulcers are associated with significant morbidity and mortality, and current treatments are far from optimal. Chronic wounds in diabetes are characterised by impaired angiogenesis, leukocyte function, fibroblast proliferation, and keratinocyte migration and proliferation.

Methods: We tested the effect of exposure to argon gas on endothelial cell, fibroblast, macrophage and keratinocyte cell cultures *in vitro* and *in vivo* of a streptozotocin-induced diabetic mouse model.

Results: Exposure to normobaric argon gas promotes multiple steps of the wound healing process. Argon accelerated angiogenesis, associated with upregulation of pro-angiogenic Angiopoietin-1 and vascular endothelial growth factor (VEGF) signalling *in vitro* and *in vivo*. Treatment with argon enhanced expression of transforming growth factor (TGF)-β, early recruitment of macrophages and keratinocyte proliferation. Argon had a pro-survival effect, inducing expression of cytoprotective mediators B-cell lymphoma 2 and heme oxygenase 1. Argon was able to accelerate wound closure in a diabetic mouse model.

Conclusion: Together these findings indicate that argon gas may be a promising candidate for clinical use in treatment of diabetic ulcers.

Key words: diabetes, wound healing, argon, angiogenesis, VEGF, TGF-β

Introduction

Diabetes mellitus is one of the greatest modern public health challenges. In diabetic patients prevalence of foot ulcers ranges from 4 to 10%, with lifetime risk of up to 25% and high recurrence rates. Over 20% of patients have poor healing of the primary ulcer and studies report 40-50% mortality rate at 5 years [1]. A major complication is lower limb amputation and diabetes accounts for 8 in 10 non-traumatic amputations, of which 85% follow a foot ulcer [2,3]. Ulcers also pose a major economic burden, with the cost of care for diabetic foot disease in England being £580 million [4]. The current management strategy for ulcers involves offloading, revascularisation, treatment of infection, and debridement [5]. Several prospective therapeutic interventions are under investigation, including novel dressing products, laser therapy, hyperbaric oxygen therapy, negative pressure therapy, cells, growth factors, and bioengineered skin grafts [6]. However, overall, the evidence for these is weak and

contradictory and current treatments are far from optimal. Given the significant personal and societal impact of ulcers, development of more effective treatments is of high priority.

The pathophysiology of diabetic foot disease is complex, involving intrinsic (neuropathy and vascular disease) and extrinsic factors (trauma, Charcot deformity, callus formation, and infection) that interact to generate a vicious cycle of pathogenicity [3,5]. Intrinsic impairments in the wound healing process lead to ulcer persistence [3,5,7]. Normal acute wound healing proceeds via four phases: coagulation, inflammation, migration-proliferation, and remodelling [5,7,8]. Macrophages, fibroblasts, endothelial cells and keratinocytes migrate to the wound site where angiogenesis and fibroblast synthesis of extracellular matrix proteins occurs, stimulated by platelet-derived growth factor (PDGF), vascular endothelial growth factor (VEGF) and transforming growth factor β (TGF-β). Closure depends on keratinocyte migration and wound contraction mediated by myofibroblasts. Temporary hypoxia after injury plays an important role, stimulating the early synthesis of growth factors, angiogenesis, and proliferation and migration of fibroblasts and keratinocytes [7]. Hypoxia inducible factor (HIF)-1α mediates the cellular adaptive response to hypoxia, upregulating expression of a host of genes, including VEGF and antioxidants such as heme oxygenase (HO)-1, resulting in a broad spectrum of protective effects [9]. Activation of the PI3K-Akt-mTOR pathway, involved in regulation of cell proliferation and survival, including expression of HIF-1α and B-cell lymphoma 2 (bcl-2), is also integral to normal wound healing [10–12].

Chronic wounds such as diabetic ulcers lose the orderly progression and synchrony of events that leads to rapid healing. Prolonged hypoxia due to vascular insufficiency causes oxidative stress, with excessive formation of reactive oxygen species (ROS), which leads to cell damage [5,8]. Cells also have impaired response to oxidative stress, as hyperglycaemia impairs the function of HIF-1α [13,14]. Hypoxia and hyperglycaemia have negative effects on neutrophil and macrophage function and vasculopathy leads to impaired recruitment of leukocytes, which predispose to wound infection [3,5,7]. There are also defects in angiogenesis, associated with reduced recruitment and dysfunction of endothelial progenitor cells, and impaired VEGF signalling [15, 16]. Compared to healthy subjects, fibroblasts isolated from diabetic ulcers show senescence and decreased proliferative response to growth factors. Derangements in migration and proliferation of keratinocytes occur, thus impairing wound re-epithelialization [5].

There are six noble gases in the atmosphere which are chemically inactive but very active biologically. Indeed, in the past decade there has been growing evidence for the cytoprotective effects of xenon and argon, although others such as helium may be cytotoxic [17–22]. Xenon protects neuronal cells [18,23], cardiac myocytes [19] and tubular kidney cells [11,12] from injury caused by oxygen-glucose deprivation *in vitro* and hypoxic-ischaemic injury *in vivo*. Recently, argon has also been shown to able to protect cells and organs from injury and promote cell survival, including *in vivo* in animal models. Argon protects rat cochlear hair cells from hypoxic and drug-induced injury [20], cardiomyocytes [24], and neuronal cells *in vitro* and *in vivo* [17,21,22,25–28]. Unlike xenon whose extraction is very costly, argon exists in high natural abundance hence is low cost and has no anaesthetic/sedative properties when administered at normobaric pressure, making it a promising safe alternative for widespread use. In addition, our previous study [22] indicated that argon is unique when compared to other noble gases in terms of a strong cell proliferation property. We, therefore, set out to investigate whether argon exposure can enhance cutaneous wound healing and assess the effect of argon on key processes (angiogenesis, cell migration), cell types (endothelial cells, fibroblasts, macrophages and keratinocytes) and signalling molecules (VEGF, angiopoietin-1, TGF-β) involved in the wound healing process both *in vitro* and in a streptozotocin (STZ)-induced diabetic mouse model.

Methods

Primary cell culture

Human umbilical vein endothelial cells (HUVECs) were cultured in EGM-2 media (EGM-2 MV bullet kit, Lonza Biosciences, UK). Fibroblasts were cultured in DMEM media (Sigma-Aldrich, Dorset, UK), supplemented with 20 nM L-glutamine (Sigma-Aldrich, UK), 10% fetal bovine serum (Thermo Scientific, Epsom, UK) and 1% penicillin/streptomycin solution (Sigma-Aldrich). THP1 (human monocyte) were cultured in RPMI1640 media (Sigma-Aldrich), supplemented with 20 nM L-glutamine, 10% fetal bovine serum and 1% penicillin/streptomycin solution. Human epidermal keratinocytes (HEK) were cultured in EpiLife Medium supplemented with Human Keratinocyte Growth Supplement (Thermo Scientific). All cells were cultured in a humidified incubator at 37°C with 5% CO_2 before experiments.

Gas exposure *in vitro*

Cells were cultured in serum-free media for 24-72 hours before being placed in a 1.5 L purpose-built, airtight, cell-culture chamber (Online supplemental Figure 1A). The gas chamber had inlet

and outlet valves and a fan to ensure equal distribution of gas within the chamber, and a sensor (Datex-Ohcmeda, Bradford, UK) to monitor the concentration of gas. The chamber was connected to calibrated flow meters to deliver the desired gas mixture (Datex gas monitor, Finland) of CO_2 (5%), oxygen (20%) and argon (75%) or nitrogen (75%) at atmospheric pressure. The cells were exposed to the gas mixtures for 2 hours at 37°C, and then returned to a standard incubator and full culture medium.

Animals

Adult male C57BL/6 mice (18-22 g) were used. Mice were given 60mg/kg of streptozotocin in 0.1 M (pH 4.5) citrate buffer by intraperitoneal injection once a day for 5 consecutive days to induce diabetes. Blood glucose levels from tail veins were measured 7 days after the fifth injection and repeated weekly. Mice with blood glucose levels above 250 mg/dL (13.9 mM) in two consecutive weeks were considered diabetic and used in subsequent experiments.

Excisional wound model

Cutaneous wound experiments were performed 4 weeks after diabetes induction. Mice were anesthetized with 2% isoflurane and 80mg/kg ketamine and dorsal skin was shaved and sanitized with 70% ethanol. Four full-thickness excisional wounds were generated with a 4 mm sterile punch (Stiefel laboratories, USA). After which, mice were exposed to either 75% argon or 75% nitrogen balanced with oxygen at atmospheric pressure with an open gas delivery system (Online supplemental figure 1B) for 2 hours once a day for 5 consecutive days.

Immunohistochemistry

For *in vitro* fluorescence staining, cells were fixed in 4% paraformaldehyde. They were incubated in 5% normal donkey serum then with rabbit anti-CD34, anti-CD68, anti-HO-1, anti-angiopoietin 1, anti-TGF-β, anti-VEGF, anti-iNOS, anti-arginase or anti-bcl-2 (all 1:200, Abcam, Cambridge, UK). Fluorochrome-conjugated or biotin-conjugated secondary antibodies were used (Millipore, Livingston, UK). For *in vivo* staining, wounded skin specimens were harvested at day 3, 5, 8, 11 and 14 after gas treatment, fixed in 4% paraformaldehyde, and embedded in paraffin. After blocking with 10% donkey serum and permeabilisation with 0.1% triton solution, sections were probed with rabbit anti-CD34 (1:100), anti-CD68 (1:100), anti-HO-1 (1:500), anti-angiopoietin 1 (1:500), anti-TGF-β (1:200), anti-VEGF (1:100), anti-iNOS (1:500) or anti-arginase (1:2000). Samples were then incubated with biotinylated secondary antibodies (1:5000) followed by avidin- HRP solution, and developed with DAB solution (0.06% DAB in 0.05M Tris/pH 7.6 with 0.03% H_2O_2). Slides were counterstained with DAPI. Immunofluorescence of cell cultures was quantified using ImageJ software (1.47v, National Institutes of Health, MD. USA) and assessed by a technician blinded to the treatment groups. Fluorescent intensity was expressed as percentages of the mean value for naïve controls. For cutaneous wound specimens, microphotographs of twenty random fields were captured using an AxioCam digital camera (Zeiss, Welwyn Garden City, UK) mounted on an Olympus BX60 microscope (Olympus, Middlesex, UK) with Zeiss KS-300 software for semi-quantitative analysis of protein expression in wound area. The number of positive staining cells per area was counted.

Western blot analysis

Protein was quantified by Bradford Protein Assay (Bio-Rad, Hemel Hempstead, UK). For protein extraction, samples (40 mg) were heated to 95°C for 10 minutes and denatured in sodium dodecyl sulphate (SDS) sample buffer (Invitrogen Ltd, Paisley, UK). The samples were loaded on a NuPAGE 4 to 12% Bis–Tris gel (Invitrogen) for electrophoresis and transferred to a PVDF membrane. The membrane was blocked using non-fat milk (Cell Signalling, Hitchin, UK) dissolved in Tris-buffered saline with Tween (TBS-T; 10 mmol Tris–HCl, 150 mmol NaCl, 0.1% Tween; pH 8.0), then probed with primary antibodies (1:1000), followed by an HRP-conjugated secondary antibody. Loading controls were α-tubulin or β-actin (1:10000, Sigma-Aldrich). Blots were visualized with the enhanced chemiluminescence (ECL) system (Santa Cruz, USA), and the protein bands were captured with GeneSnap and analysed using GeneTools software (Syngene, Cambridge, UK).

In vitro angiogenesis assay

Angiogenesis was analysed using endothelial tube formation assay (Invitrogen, UK), following the manufacturer's instructions. Plates (96-well) were coated with Matrigel and HUVECs were seeded at a density of 1×10^4 per well. HUVECs were treated with 75% argon or 75% nitrogen for 2 hours then replaced in a standard incubator for 4 hours. Tube formation was assessed at 2, 4, 6 and 8 hours after seeding using a phase-contrast microscope (Olympus CK30, Tokyo, Japan); the number of tubes in 10 fields was counted.

Scratch assay

Scratch assay was performed to assess HUVEC and fibroblast cell migration. When 90% confluence was reached, cells were cultured in serum free medium overnight and one artificial gap per well was scratched with a sterile plastic 1 ml micropipette tip to generate a uniform gap that was devoid of adherent

cells. Cells were exposed to 75% argon or 75% nitrogen for 2 hours then returned to standard conditions. Gap closure was monitored using a phase-contrast microscope and defined as the mean percentage of the remaining cell-free area 24 hours after treatment compared with the initial wound area.

MTT assay

MTT assay was performed 24 hours after gas exposure. Cells were incubated in 100 µL of 0.5 mg/mL 3-(4, 5-dimethylthiazol-2-yl) 2, 5-diphenyltetrazolium bromide (MTT) solution (CPLbiochem, UK) for 2 hours at 37°C, and then 100 µL dimethyl sulfoxide (DMSO) (Fischer, UK) for 10 minutes at room temperature. Optical densities (OD) of cell cultures were measured at 595nm spectrophotometrically with a microplate reader (MRX II, Dynex technologies, UK) and values normalised to control.

Trypan blue assay

Trypan blue assay was performed 24 hours after gas exposure. Cells were dissociated with 0.25% trypsin-EDTA solution and re-suspended in EGM. 10 µL of each sample was mixed with an equal volume of trypan blue dye (Sigma-Aldrich) and pipetted onto a haemocytometer slide. The proportion of blue-staining cells were counted to determine the % cell death in each group.

Assessment of macroscopic wound healing

Photographs of each wound were taken at the indicated time points post-gas exposure and analyzed using Image J (NIH, Bethesda, Maryland, USA).

Statistics

All data are presented as mean ± SD. Data were analysed with ANOVA followed by *post hoc* Tukey comparison. For two group comparison, two-tailed unpaired t-tests were used to determine the significances. A $p < 0.05$ was considered to be statistically significant.

Ethics approval

All animal experiments were approved by the Animal Study Committee of Third Military Medicine University, Chongqing, China (N201203056) and conducted in accordance with the UK Animals (Scientific Procedures) Act 1986. All procedures are also compliant with the ARRIVE guidelines for reporting animal experiments.

Results

Argon promoted angiogenesis

In vitro endothelial tube formation assay was used to assess the effect of argon on endothelial cell differentiation. The number of tubes formed by HUVECs was enhanced when cells were exposed to 75% argon compared to 75% nitrogen (p=0.0001) and the negative control (NC) group (p=0.0001) at 2 and 4 hours post-exposure (Figure 1A). Although there was enhanced tube formation in the nitrogen-exposed group at 6 hours, the argon group was still significantly higher than nitrogen (p=0.001) and NC (p=0.0001) at this time point. The effect of argon appeared to diminish over time although the same trend was observed in the positive control group.

We investigated whether argon could have the same effect *in vivo* in a diabetic chronic wound environment, using a mouse model well established in previous studies of impaired would healing in diabetes [29]. Consistent with *in vitro* observations, immunostaining for CD34, a marker of new vessel growth, indicated that there was increased blood vessel density in animals in the argon-exposed group compared to the nitrogen-exposed group at day 3 (p=0.0015) and 5 after injury (p=0.0071) (Figure 1B). These results suggest that argon promotes early angiogenesis, driving rapid formation of granulation tissue, during wound healing.

Argon promoted cell migration

Exposure to argon accelerated HUVEC and fibroblast migration compared to the nitrogen-treated groups (HUVEC, p=0.0002; fibroblast, p=0.0055) (Figure 1C-D). Cell migration underlies angiogenesis and fibroplasia, hence this suggests beneficial effects of argon on speed of wound healing.

Argon stimulated angiogenic signalling

During wound healing the key drivers of angiogenesis are basic fibroblast growth factor (bFGF, initiates angiogenesis in the first three days) and VEGF (critical for angiogenesis from day 4 to 7). Other factors with angiogenic activity include TGF-β and angiopoietin-1, which stimulate production of bFGF and VEGF by macrophages and endothelial cells [7]. We hypothesised that the beneficial effect of argon on angiogenesis might correlate with upregulation of pro-angiogenic factors. Treatment of cultured fibroblasts with argon increased angiopoietin-1 expression, as shown by immunofluorescence staining (p=0.0004) and Western blot analysis (p=0.0002) (Figure 2A-B). Angiopoietin-1 protein expression was markedly increased in cutaneous wounds of argon-treated mice at 3 days after injury ($p< 0.05$) (Figure 2C).

Furthermore argon augmented VEGF expression in cells (Figure 2D-E) and skin wounds of diabetic mice (Figure 2F). Altogether, these data provide evidence that argon can promote angiogenesis in skin wounds in diabetes.

Argon treatment induced upregulation of TGF-β and improved organisation of α smooth muscle actin (α-SMA) in fibroblasts

Fibroblast proliferation and synthesis of matrix proteins under the stimulation of growth factors such as TGF-β1, PDGF, FGFs and VEGF, is a key component of the proliferation phase of wound healing and implicated in the pathogenesis of diabetic foot ulcers [5,7]. Argon induced TGF-β expression in human fibroblasts (Figure 3A-B) and increased levels of TGF- β in wounds of diabetic mice, although a significant effect was only seen at day 5 (Figure 3C).

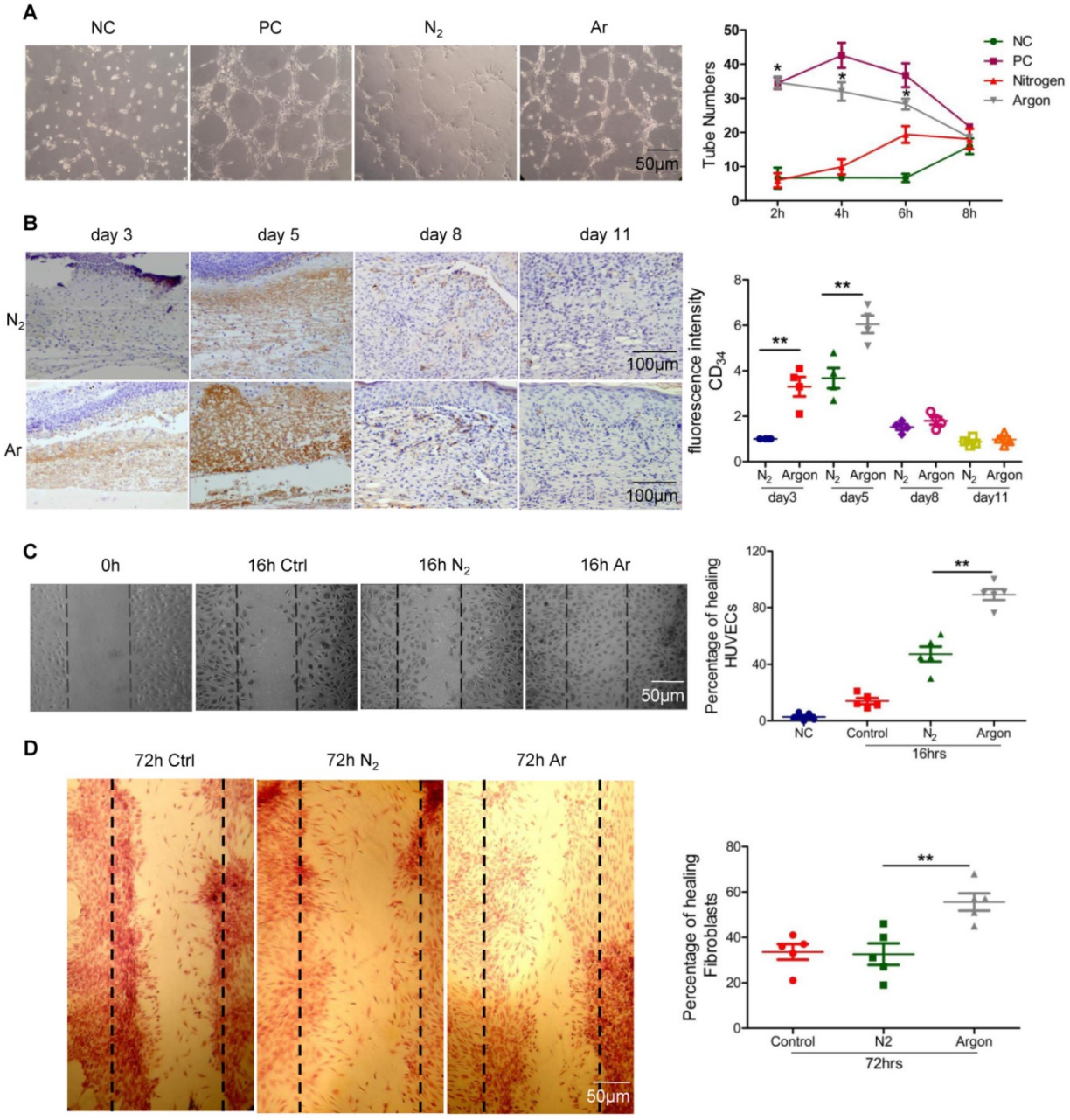

Figure 1. Argon exposure accelerated angiogenesis *in vitro* and *in vivo* and cell migration *in vitro*. (**a**) HUVECs were seeded on growth factor reduced Matrigel and incubated in serum-free medium with (PC) or without 5 ng/ml FGF (NC, N2 and Argon), and exposed to room air (controls), nitrogen gas (20% O2 + 5% CO2 + 75% N2) or argon gas (20% O2 + 5% CO2 + 75% Ar) for 2 hours and then room air for 4 hours. Left: Pictures were taken at 2 hours after seeding. Representative images of six independent experiments each performed in triplicate are shown. Right: The number of tubes was counted in 10 fields/well at 2, 4, 6 and 8 hours after seeding. (**b**) Mice were exposed to nitrogen (25% O2 + 75% N2) or argon gas (25% O2 + 75% Ar). Left: CD34 expression in mouse cutaneous wounds was detected by immunohistochemistry. Cells were counterstained with DAPI (blue). Right: Fluorescent intensity of CD34 was quantified by densitometry and normalized to N_2 at day 3 (n=12). (**c**) HUVECs were grown on collagen-coated plastic dishes. The cultures were wounded as described and exposed to room air (control), nitrogen gas (20% O2 + 5% CO2 + 75% N2) or argon gas (20% O2 + 5% CO2 + 75% Ar). Left: Pictures were taken at 16 hours after wounding of HUVECs. Representative images of six independent experiments are shown. Right: Percentage of wound closure (gap closure) at 16 hours after seeding in low-power microscopic fields (x20) in 6 wells was measured. (**d**) Fibroblasts were grown on collagen-coated plastic dishes. Left: Pictures were taken at 72 hours after wounding of fibroblasts. Representative images of six independent experiments are shown. Right: Percentage of wound closure (gap closure) at 72 hours after seeding in low-power microscopic field (x20) in 6 wells was measured. Data are means ± S.D.; *P<0.05, **P<0.01. NC, negative control; PC, positive control.

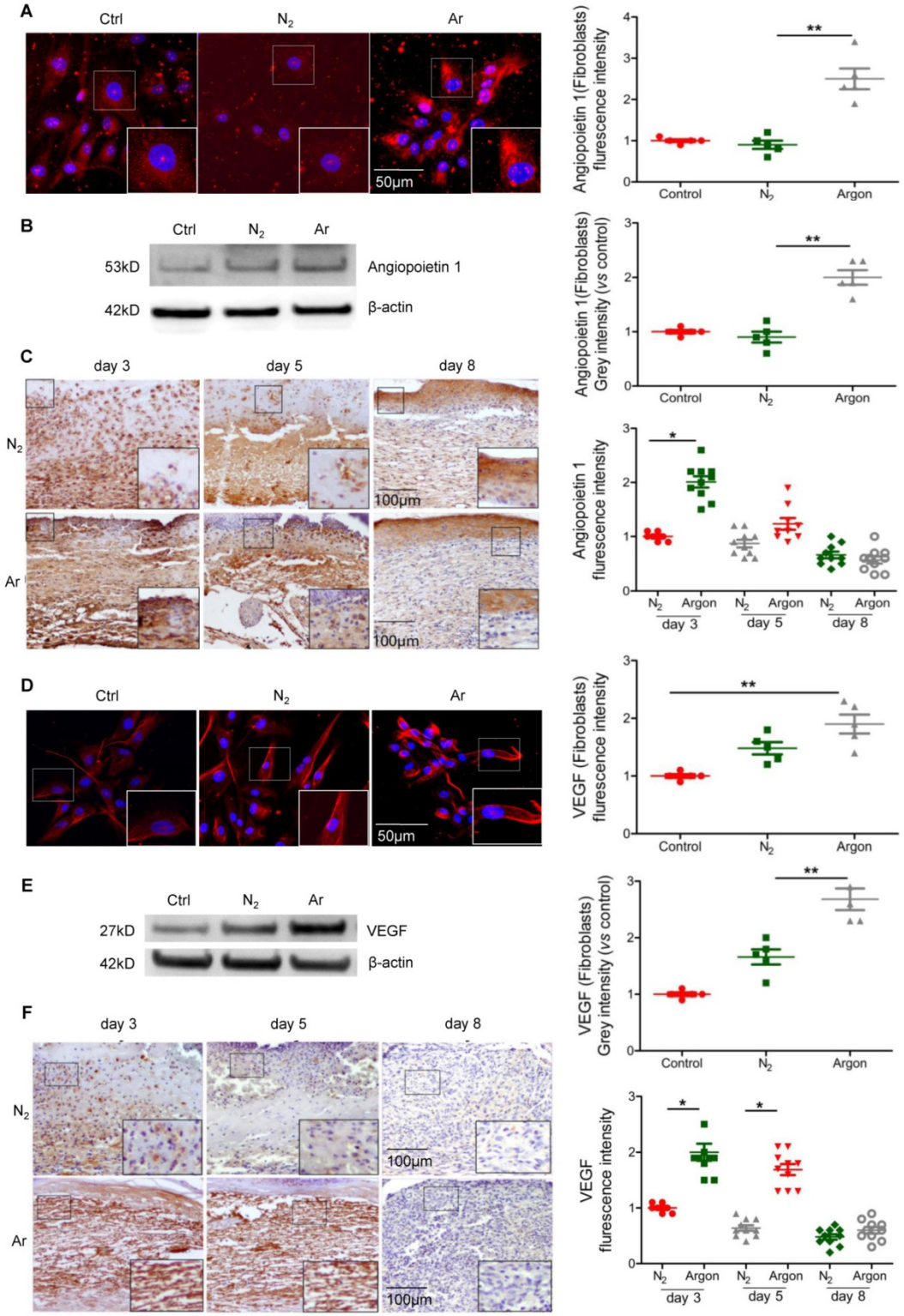

Figure 2. Argon exposure enhanced expression of Angiopoietin-1 and VEGF *in vitro* and *in vivo*. (**a**) Fibroblasts were incubated in DMEM/low glucose media containing 10% FBS and exposed to room air (control), nitrogen gas (20% O2 + 5% CO2 + 75% N2) or argon gas (20% O2 + 5% CO2 + 75% Ar). Left: Angiopoietin-1 expression (red) in fibroblasts was detected by immunofluorescence staining at 24 hours after gas exposure. Cells were counterstained with DAPI (blue). Right: fluorescent intensity of Angiopoietin-1 was normalized to control (n=6). (**b**) Left: Angiopoietin-1 expression in fibroblasts was detected by western blotting. Right: intensity of Angiopoietin-1 was quantified by densitometry and normalized to control (n=5). (**c**) Mice were exposed to nitrogen (25% O2 + 75% N2) or argon gas (25% O2 + 75% Ar). Left: Angiopoietin-1 expression in mouse cutaneous wounds was detected by immunohistochemistry. Representative images at 3, 5 and 8 days after injury are shown. Right: fluorescent intensity of Angiopoietin-1 was quantified by densitometry and normalized to N_2 at day 3 (n=10). (**d**) Left: VEGF expression (red) in fibroblasts was detected by immunofluorescence staining at 24 hours after gas exposure. Cells were counterstained with DAPI (blue). Right: fluorescent intensity of VEGF was normalized to control (n=5). (**e**) Left: VEGF expression in fibroblasts was detected by western blotting. Right: intensity of VEGF was quantified by densitometry and normalized to control (n=5). (**f**) Left: VEGF expression in mouse cutaneous wounds was detected by immunohistochemistry. Representative images at 3, 5 and 8 days after injury are shown. Right: fluorescent intensity of VEGF was quantified by densitometry and normalized to N_2 at day 3 (n=10). Data are means ± S.D.; *P<0.05, **P<0.01.

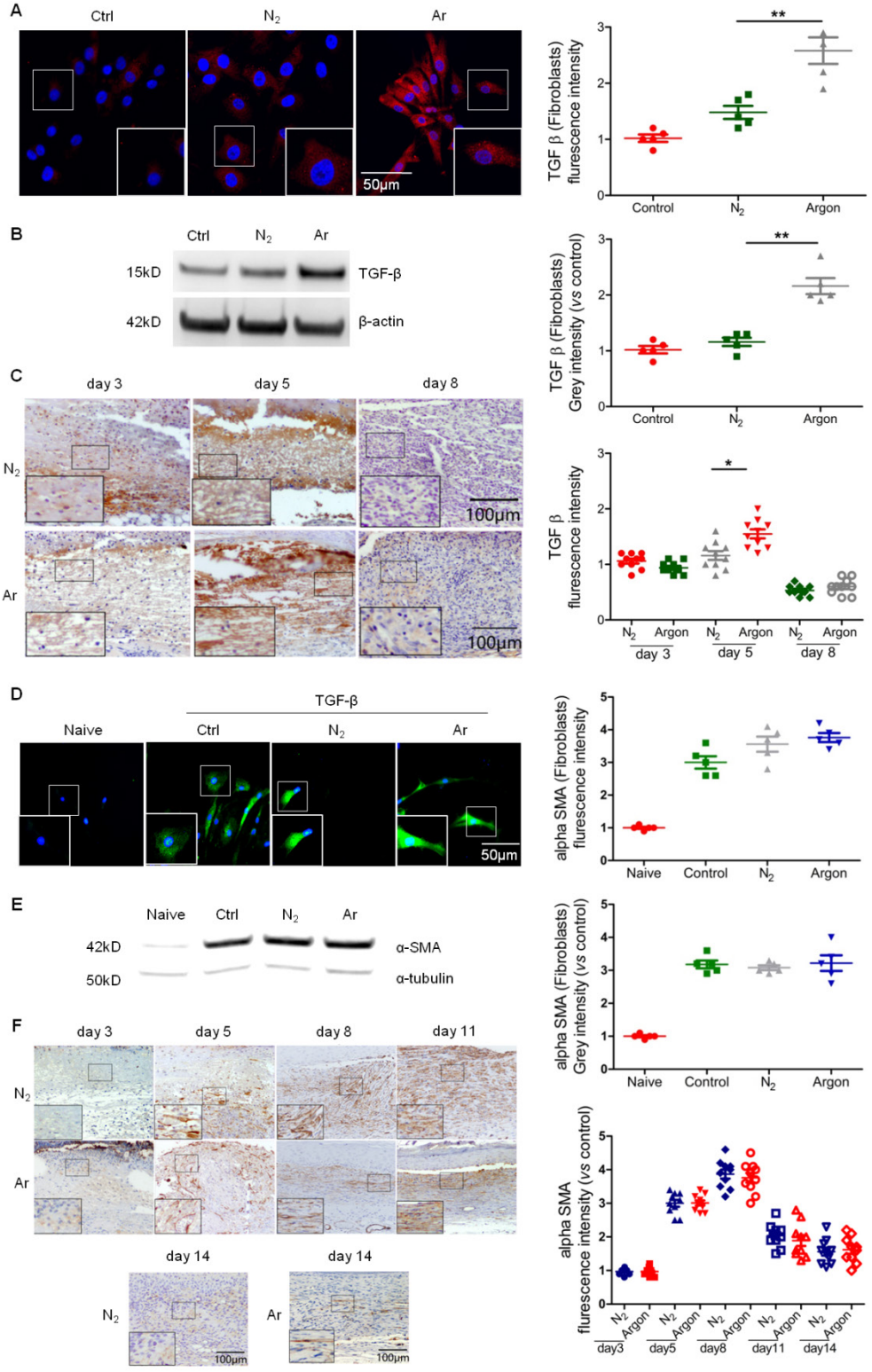

Figure 3. Argon enhanced TGF-β expression *in vitro* and *in vivo* and improved α-SMA organisation *in vivo*. (**a**) Fibroblasts were incubated in DMEM/low glucose media containing 10% FBS and exposed to room air (control), nitrogen gas (20% O2 + 5% CO2 + 75% N2) or argon gas (20% O2 + 5% CO2 + 75% Ar). Left: TGF-β expression (red) in fibroblasts was detected by immunofluorescence staining at 24 h after gas exposure. Cells were counterstained with DAPI (blue). Right: fluorescent intensity of TGF-β was normalized to control (n=5). (**b**) Left: TGF-β expression in fibroblasts was detected by western blotting. Right: intensity of TGF-β was quantified by densitometry and normalized to control (n=6). (**c**) Mice were exposed to nitrogen (25% O2 + 75% N2) or argon gas (25% O2 + 75% Ar). Left: TGF-β expression in mouse cutaneous wounds was detected by immunohistochemistry. Representative images at 3, 5 and 8 days after injury are shown. Right: fluorescent intensity of TGF-β was quantified by densitometry and normalized to N_2 at day 3 (n=10). (**d**) Fibroblasts were incubated in DMEM/low glucose media containing 10% FBS without (Naive) or with (Control, N2 and Argon) 10 ng/ml TGF-β. Cells were exposed to room air (control), nitrogen gas (20% O2 + 5% CO2 + 75% N2) or argon gas (20% O2 + 5% CO2 + 75% Ar). Left: α-SMA expression (green) in fibroblasts was detected by immunofluorescence staining at 72 hours after gas exposure. Cells were counterstained with DAPI (blue). Right: fluorescent intensity of α-SMA was normalised to naïve (n=5). (**e**) Left: α-SMA expression in fibroblasts was detected by western blotting. Right: intensity of α-SMA was quantified by densitometry and normalized to naïve (n=6). (**f**) Top: α-SMA expression in mouse cutaneous wounds was detected by immunohistochemistry. Representative images at 3, 5, 8, 11 and 14 days after injury are shown. Bottom: fluorescent intensity of α-SMA was quantified by densitometry and normalized to N_2 at day 3 (n=10). Data are means ± S.D.; *P<0.05, **P<0.01.

A key TGF-β-mediated response is differentiation of fibroblasts to myofibroblasts, characterized by large bundles of actin-containing microfilaments, which are responsible for wound contraction. Impaired wound healing in diabetic ulcers is associated with failure of timely contraction [5,7,8]. To investigate whether argon has an effect on myofibroblast development, we treated fibroblasts with TGF-β to induce phenotype change, before conditioning with argon. Immunostaining showed that α-SMA expression was increased in TGF-β-treated cells compared to naïve, confirming successful induction of fibroblast-myofibroblast differentiation, but there were no significant differences in α-SMA expression between the argon and control groups (Figure 3D-E). Similarly, argon had no effect on α-SMA expression *in vivo* (Figure 3F). However, α-SMA showed more organised arrangement in argon-treated wounds, seen at day 5 and 8 (Figure 3F). This was associated with enhanced quality of wound healing and reduction of scar formation.

Argon exposure increased macrophage recruitment and activity

A major factor contributing to poor healing of diabetic ulcers is dysregulation of inflammatory responses to injury with prolonged inflammation and hyperproduction of proinflammatory cytokines [5,30]. Argon increased the recruitment of CD68+ macrophages into the wound site in the early stages of wound healing (Figure 4A). Argon also influenced macrophage phenotype. Upregulation of inducible nitric oxide synthase (iNOS), a marker of the pro-inflammatory M1 phenotype, was observed in THP-1 cells treated with argon. There was no change in expression of arginase (M2 phenotype marker) (Figure 4B). This suggests that argon promotes differentiation of monocytes to M1 macrophages. Similarly, there were increased iNOS+ cells early after injury in diabetic skin wounds after argon exposure and no significant difference in numbers of arginase+ cells between the nitrogen- and argon-treated groups (Figure 4C-D).

Argon promoted proliferation of keratinocytes

Reepithelialization is essential for wound closure and involves epidermal cell migration and, for larger wounds, keratinocyte proliferation [5,7]. Argon increased the proportion of proliferating HEKs in culture (Figure 5A). However the physiological relevance of this is uncertain. Analysis of the expression of filaggrin, a keratin-binding protein that is an epithelial cell marker, showed no differences between nitrogen- and argon-treated wounds from day 8 to 14 (Figure 5B).

Treatment with argon improved survival of endothelial and fibroblast cells

Argon increased endothelial cell viability assessed with MTT assay ($p=0.0013$) (Figure 6A). We also observed a trend towards a reduced cell death in argon-treated cultures but this did not reach statistical significance ($p=0.057$) (Figure 6B). As previous studies have shown that xenon and argon can inhibit apoptosis in rodent models of neural and renal injury [12,25], we investigated whether improved cell survival after argon exposure was associated with upregulation of bcl-2 and HO-1. Immunofluorescence analysis showed that expression of bcl-2 was increased in argon-treated cells at 4 and 24 hours post-exposure relative to the controls (Figure 6C). Similarly, expression of HO-1 was enhanced in argon-treated HUVECs and fibroblasts (Figure 6D-E).

Argon accelerated cutaneous wound healing in diabetic mice

Wound gross morphology and closure were assessed at several timepoints. After 14 days, there was essentially full closure of wounds in argon-treated animals. Argon-treated animals had significantly smaller wounds at day 5, 7, 9, 11 and 14 after injury compared to control (Figure 7A-B).

Discussion and Conclusions

In this study we found that argon exposure had positive effects on multiple processes involved in wound repair. It enhanced angiogenesis and cell migration, increased recruitment of macrophages and altered macrophage phenotype, enhanced function of myofibroblasts, and increased keratinocyte proliferation. Expression of VEGF, angiopoietin-1, TGF-β, HO-1 and bcl-2 were markedly increased following treatment. Consequently, cutaneous wound healing in diabetic mice was improved.

There is much interest in biologic agents designed to modify deranged molecular and cellular biology underlying impaired wound healing, including growth factors VEGF [31,32] and PDGF [33], bioengineered skin grafts, and autologous mesenchymal stem cells [6]. However, results have been mixed and often show low efficacy, likely because optimal healing requires a multidimensional approach tackling numerous issues present such as inadequate angiogenesis, impaired fibroblast responses and immune dysfunction. Another area of interest in chronic wound management is application of non-thermal atmospheric-pressure plasma, including that of argon. Studies have shown that plasma treatment can promote wound healing, possibly through antibacterial effects, enhancement of angiogenesis, and stimulation of fibroblast, endothelial cell and

keratinocyte proliferation [34–37], including in chronic and diabetic wounds [38,39], and in a few clinical trials [40–42]. However, there exist issues with the use of plasma, such as the lack of standardisation of characterization of plasma physical characteristics and biological performance and definition of plasma parameters, in the face of a wide variety of plasma devices and sources [43,44]. Studies have found differing effects of plasma on cell viability, cell proliferation and apoptosis dependent upon the specific plasma source, treatment regimen and duration, and time post-exposure of investigation [43,45,46].

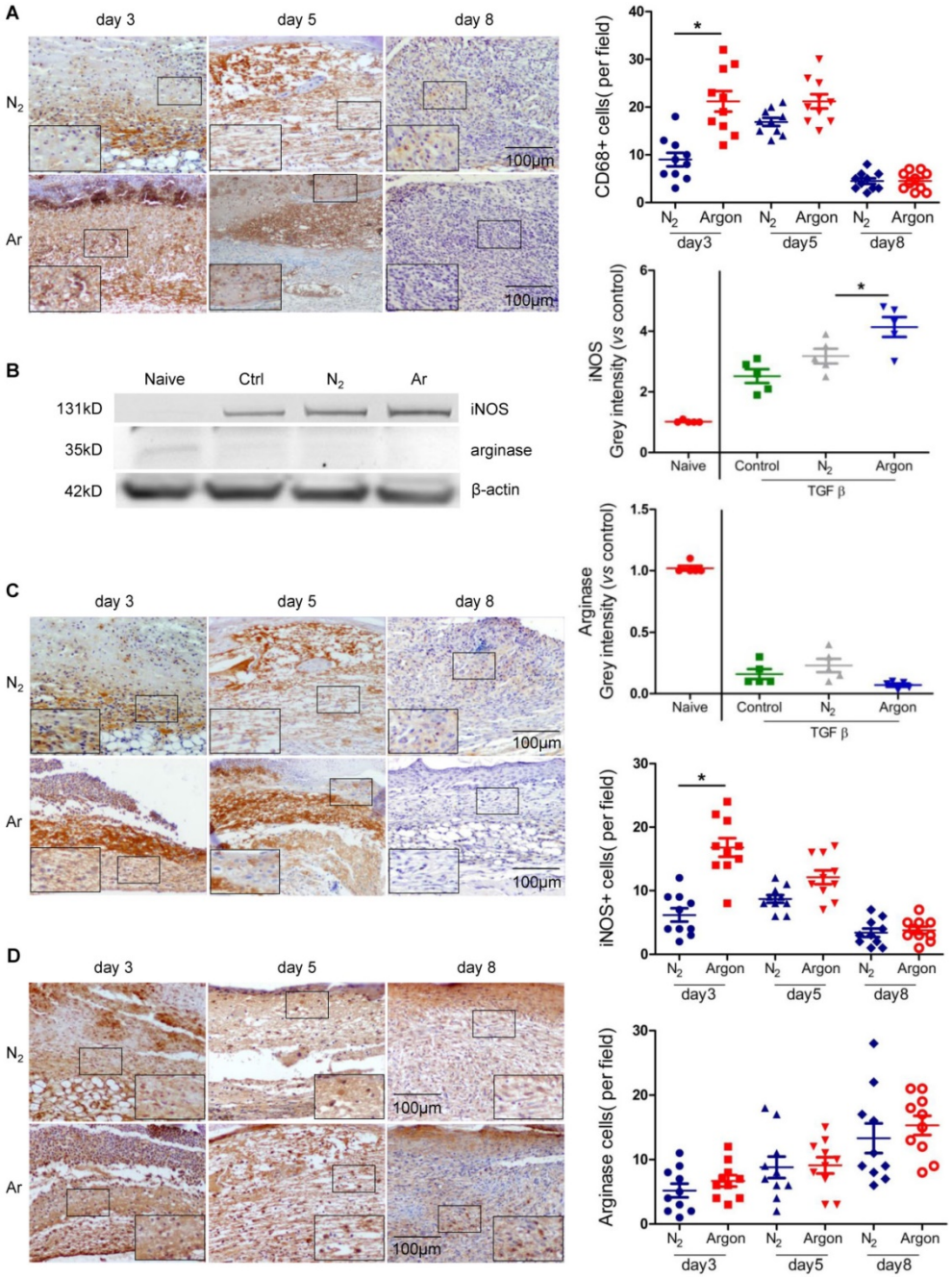

Figure 4. Argon enhanced human macrophage recruitment and polarization to M1 phenotype *in vitro* and *in vivo*. (**a**) Mice were exposed to nitrogen (25% O2 + 75% N2) or argon gas (25% O2 + 75% Ar). Left: CD68 expression in mouse cutaneous wounds was detected by immunohistochemistry. Representative images at 3, 5 and 8 days after injury are shown. Right: the number of CD68+ cells per 100x magnification field in 10 fields was counted (n=10). (**b**) THP1 were incubated in RPMI1640 containing 10% FBS without (Naïve) or with 10 ng/ml TGF-β (Control, N2 and Argon). Cells were exposed to room air (control), nitrogen gas (20% O2 + 5% CO2 + 75% N2) or argon gas (20% O2 + 5% CO2 + 75% Ar). Left: inducible nitric oxide synthase (iNOS, marker of M1 macrophage) and arginase (marker of M2 macrophage) expression in THP1 was detected by western blotting. Right: intensity of iNOS and arginase was quantified by densitometry and normalized to naïve (n=5). (**c**) Left: iNOS expression in mouse cutaneous wounds was detected by immunohistochemistry. Representative images at 3, 5 and 8 days after injury are shown. Right: the number of iNOS+ cells per 100x magnification field in 10 fields was counted (n=10). (**d**) Left: arginase expression in mouse cutaneous wounds was detected by immunohistochemistry. Representative images at 3, 5 and 8 days after injury are shown. Right: the number of arginase+ cells per 100x magnification field in 10 fields was counted (n=10). Data are means ± S.D.; *P<0.05.

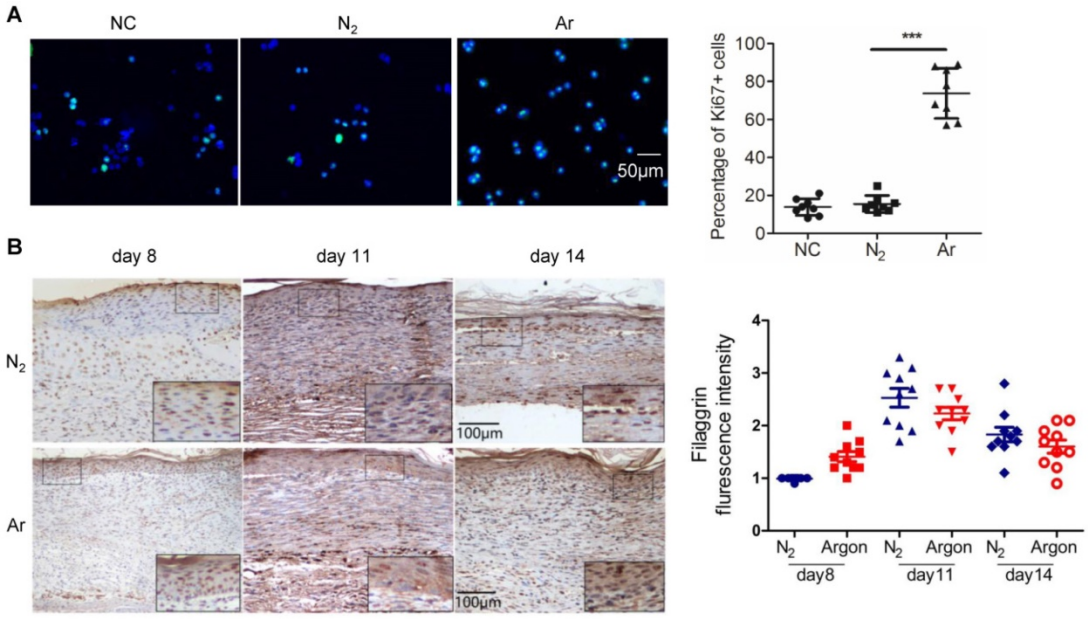

Figure 5. Argon enhanced human keratinocyte proliferation but had no significant effect on filaggrin expression *in vivo*. (**a**) Keratinocytes were incubated in EpiLife media and exposed to room air (control), nitrogen gas (20% O2 + 5% CO2 + 75% N2) or argon gas (20% O2 + 5% CO2 + 75% Ar). Left: Ki-67 expression (green) in keratinocytes was detected by immunofluorescence staining at 24 hours after gas exposure. Cells were counterstained with DAPI (blue). Right: the number of Ki-67+ cells per 100x magnification field in 10 fields was counted and percentage of Ki-67+ cells was determined (n=8). (**b**) Mice were exposed to nitrogen (25% O2 + 75% N2) or argon gas (25% O2 + 75% Ar). Left: filaggrin expression in mouse cutaneous wounds was detected by immunohistochemistry. Representative images at 8, 11 and 14 days after injury are shown. Right: fluorescent intensity of filaggrin was quantified by densitometry and normalized to N2 at day 8 (n=10). Data are means ± S.D. ***P<0.001.

Diabetes mellitus is associated with abnormal angiogenesis. This may be due to decreased VEGF expression, as a result of hyperglycaemia-induced decrease in transactivation of HIF-1α [14], lipid peroxidation [47], or insulin resistance [16]. Under-expression of TGF-β1 and bFGF, both capable of inducing VEGF, may contribute to impaired angiogenic response [16]. There may also be insufficient recruitment and defective function of endothelial progenitor cells (EPCs) [15]. Our study suggested that argon can rescue defective angiogenesis in diabetic wounds. We found an increase in the number of CD34+ endothelial progenitor cells in wounds after argon treatment. Early expression of VEGF was also increased by argon. This agrees with previous studies showing argon and xenon upregulate VEGF [24,48]. The significance of this is highlighted by findings in diabetic mice that topical VEGF increased EPC recruitment, granulation tissue formation, and matrix deposition and epithelialization, leading to accelerated repair [31]. In addition, argon enhanced expression of angiopoietin-1, an important regulator of vascular development, inflammation and wound healing [49]. This may contribute to the observed improvement in angiogenesis as angiopoietin-1 or its derivatives are known to promote angiogenesis in a VEGF-independent manner [50,51]. Angiopoietin-1 may also have positive effects on mobilization of EPCs from bone marrow, and wound re-epithelialization [52].

In this study argon enhanced migration of endothelial cells and fibroblasts. Cells from chronic wounds show reduced migration, possibly related to dysregulated connexin 43, JNK signalling or fibronectin [53,54]. The effect of argon on these signalling pathways and processes should be investigated in future studies.

TGF-β has a central role in wound healing, and reduced TGF-β signalling contributes to non-healing wounds in diabetes [55]. We found that argon induced upregulation of TGF-β in fibroblasts. It has been suggested that glucose-mediated depression of signalling through the TGF-β/Smad pathway leads to impaired myofibroblast differentiation. Although there was no change in level of α-SMA, argon promoted better organisation of α-SMA in myofibroblasts, which may have contributed to improved quality of wound healing, and thus has potential important clinical implications.

Chronic inflammation is a hallmark of diabetic wounds. A substantial body of evidence suggests that this is associated with impaired transition of macrophages from pro-inflammatory M1 to anti-inflammatory M2 phenotype [29,30,56]. M1 macrophages usually appear in early stages of healing (up to day 5) and phenotypic switch occurs with progression of healing such that M2 macrophages predominate in the later proliferative stage (day 10) [57]. Persistence of pro-inflammatory macrophages is associated with reduced expression of VEGF and

TGF-β1 [29]. These findings appear to contradict the results of this study, which showed that argon increased the numbers of M1 macrophages and had no effect on M2 macrophages in diabetic wounds. However, upregulation of pro-inflammatory macrophages only occurred early (at day 3) after injury, when macrophages usually exhibit M1 phenotype in normal wounds, so it may be the case that the argon-induced boost in early pro-inflammatory macrophages is beneficial for wound healing. Supporting this hypothesis, a study in a STZ-induced diabetic rat model [58] showed that diabetic wounds had insufficient M1 macrophages in the initial stage of healing. Furthermore, application of M2 macrophages does not improve but rather delays wound healing, which suggests M1 macrophages perhaps have important functions in early repair [59]. One possibility is that increased macrophage activity protects against infection, a major cause of non-healing.

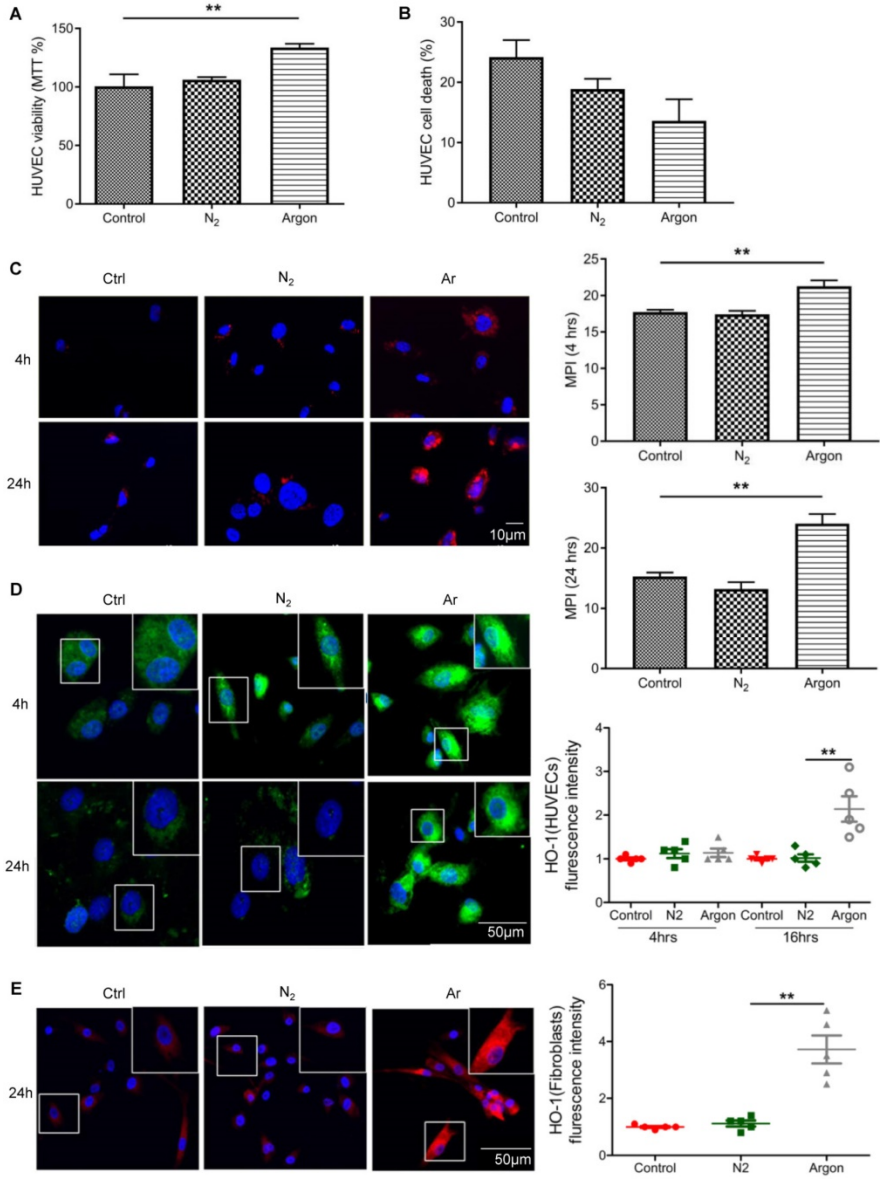

Figure 6. Argon exposure enhanced survival, bcl-2 and haem oxygenase (HO)-1 expression in HUVECs and fibroblasts. HUVECs were incubated in endothelial growth medium (EGM) containing 2% FBS and fibroblasts were incubated in DMEM/low glucose media containing 10% FBS. Cells were exposed to room air (control), nitrogen gas (20% O2 + 5% CO2 + 75% N2) or argon gas (20% O2 + 5% CO2 + 75% Ar) for 2 hours. (**a**) HUVEC survival at 24 hours after gas exposure was determined by MTT assay and normalized to control (n=3). (**b**) Percentage HUVEC death at 24 hours after gas exposure was determined by trypan blue assay at 100x magnification (n=4). (**c**) Left: bcl-2 expression (red) in HUVECs was detected by immunofluorescence staining at 4 and 24 hours after gas exposure. Cells were counterstained with DAPI (blue). Right: fluorescent intensity of bcl-2 was determined from 5 images per group and expressed as MPI (n=4). (**d**) Left: HO-1 expression (green) in HUVECs was detected by immunofluorescence staining at 4 and 24 hours after gas exposure. Cells were counterstained with DAPI (blue). Right: fluorescent intensity of HO-1 in HUVECs was normalized to control (n=4). (**e**) Left: HO-1 expression (red) in fibroblasts was detected by immunofluorescence staining at 24 hours after gas exposure. Cells were counterstained with DAPI (blue). Right: fluorescent intensity of HO-1 in fibroblasts normalized to control (n=4). Data are means ± S.D.; **P<0.01.

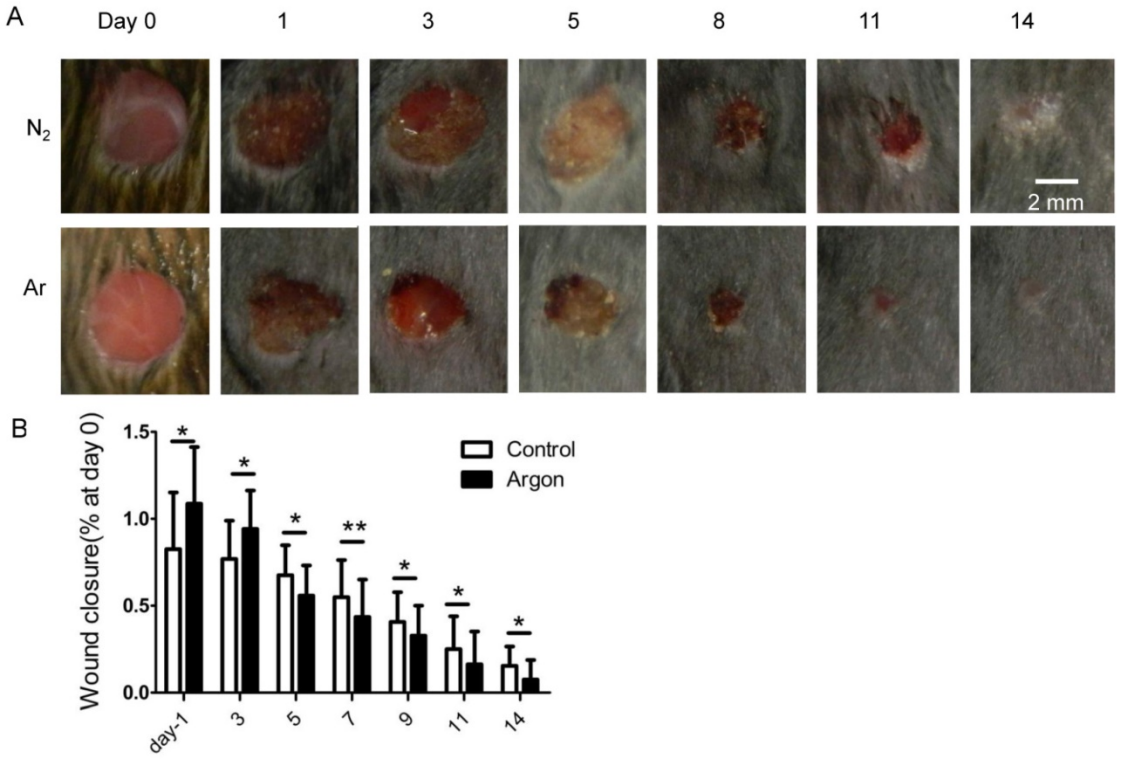

Figure 7. Effect of argon exposure on skin wound healing in mice. (**a**) Macroscopic changes in skin wound site in mice exposed to nitrogen (25% O2 + 75% N2) or argon gas (25% O2 + 75% Ar). The day 0 picture was taken immediately after injury. Representative images from 2 individual animals in both groups are shown. (**b**) Percentage remaining wound area (wound area/the original wound area) at each time point (n=12). Data are means ± S.D.; *P<0.05, **P<0.01.

In diabetic wounds, hyperglycaemia and excess oxidative stress impair keratinocyte proliferation and survival [8]. We demonstrated that argon could increase proliferation of human keratinocytes. We did not see an enhancement of reepithelialisation but this may have been because the effect of argon occurred early, before the period of time that we studied (day 8 to 14).

Enhanced wound healing by argon involves upregulation of HO-1. HO-1 is a cytoprotective enzyme maximally expressed at days 2 to 3 post-injury, which has a critical role in protection of cells from ROS [8,60]. It is also involved in upregulation of VEGF [61]. Induction of HO-1 is reduced and delayed in diabetic chronic wounds, which are characterised by high oxidative stress, and HO-1 augments endothelial cell proliferation and capillary formation in angiogenic assay *in vitro* and can improve wound healing in a diabetic mouse model [60,61]. Our results show argon upregulates HO-1, consistent with previous studies of the cytoprotective mechanisms of argon in retinal ganglion cells, cortical neuronal cells and rat hippocampus [26–28]. Argon also increased bcl-2 expression consistent with previous reports of xenon in protection of brain and kidney [62,63]. Apoptosis may be an important target as diabetic wounds have high levels of apoptosis compared to normal acute wounds, with significantly enhanced caspase-8, -9, and -3 activity and low bcl-2 expression [64].

Our study is not without limitations. We have only used a single mouse model. The effect of argon might also be studied in the *db/db* diabetic mouse, the most commonly used model for human chronic diabetic wounds. Secondly, we only investigated the effect of one treatment regime, and, as the optimal concentration and exposure duration is unknown, this should be further explored. Furthermore, our data shows the mechanisms of argon action are enhancement of cell viability and prevention of apoptosis through upregulation of antioxidant proteins such as HO-1 and/or anti-apoptotic mediators e.g. bcl-2, which has been consistently demonstrated in previous studies of argon gas [17,25–28]. Previous studies suggest regulation of HO-1 may involve signalling through ERK-1/2, whose expression is induced by argon, or HIF-1α [26,28], and that the protective effect of argon may be partly due to upregulation of the PI3K-Akt pathway [27]. However, the main objective of this study was proof-of-concept, and further studies are required to elucidate the full mechanism of argon action.

In this study, we showed that a relatively short and low-intensity regime was effective in accelerating wound healing in a clinically relevant diabetic mouse model. Furthermore, argon has a good safety profile,

few side effects, rapid onset of action, and is relatively inexpensive. In addition, unlike ordinary drugs, a unique advantage of gas treatment, e.g. argon, is that it does not require "good" blood flow and is ready to penetrate and reach regions including diabetic wounds with compromised blood supply. Together, our data suggest that argon may be a promising candidate for use in clinical management of diabetic ulcers, although further studies to investigate optimum concentration or administration route *vs* efficacy is warranted, before it can proceed to clinical trials.

Abbreviations

α-SMA: α smooth muscle actin; Bcl-2: B-cell lymphoma 2; bFGF: basic fibroblast growth factor; HEK: human epidermal keratinocyte; HIF-1α: hypoxia inducible factor-1α; HO-1: heme oxygenase-1; HUVEC: human umbilical vein endothelial cell; iNOS: inducible nitric oxide synthase; PDGF: platelet-derived growth factor; STZ: streptozotocin; TGF-β: transforming growth factor β; VEGF: vascular endothelial growth factor.

Supplementary Material

Supplementary figures and tables.
http://www.thno.org/v09p0477s1.pdf

Acknowledgements

The study was supported by the collaborative grants between DM and KL and grants from BJA/RCoA, London, UK (to DM) and the National Natural Science Foundation of China (grant no. 81470267).

Author contributions

JN, HZ, KL and DM designed the study. JN, HZ, BC, ZY, WQ and KWJL conducted the experiments. JN, HZ, EM, VB, TI and DM analysed and interpreted data. JN, HZ, EM and DM wrote the manuscript. All authors reviewed and have approved the final manuscript.

Competing Interests

VB and TI are management and shareholders of Nobilis Therapeutics, a biotechnology company developing therapeutics based on noble gas administration. DM is a shareholder and scientific advisory board member of Nobilis Therapeutics. All other authors have no competing interests.

References

1. Morbach S, Furchert H, Gröblinghoff U, Hoffmeier H, Kersten K, Klauke G-T, et al. Long-term prognosis of diabetic foot patients and their limbs: amputation and death over the course of a decade. Diabetes Care. 2012; 35: 2021–7.
2. Boulton AJ, Vileikyte L, Ragnarson-Tennvall G, Apelqvist J. The global burden of diabetic foot disease. Lancet. 2005; 366: 1719–24.
3. Singh N, Armstrong DG, Lipsky BA. Preventing Foot Ulcers in Patients With Diabetes. JAMA. 2005; 293: 217.
4. Kerr M, Rayman G, Jeffcoate WJ. Cost of diabetic foot disease to the National Health Service in England. Diabet Med. 2014; 31: 1498–504.
5. Falanga V. Wound healing and its impairment in the diabetic foot. Lancet. 2005; 366: 1736–43.
6. Game FL, Apelqvist J, Attinger C, Hartemann A, Hinchliffe RJ, Löndahl M, et al. Effectiveness of interventions to enhance healing of chronic ulcers of the foot in diabetes: a systematic review. Diabetes Metab Res Rev. 2016; 32: 154–68.
7. Epstein FH, Singer AJ, Clark RAF. Cutaneous Wound Healing. N Engl J Med. 1999; 341: 738–46.
8. Schafer M, Werner S. Oxidative stress in normal and impaired wound repair. Pharmacol Res. 2008; 58: 165–71.
9. Pugh CW, Ratcliffe PJ. Regulation of angiogenesis by hypoxia: role of the HIF system. Nat Med. 2003; 9: 677–84.
10. Squarize CH, Castilho RM, Bugge TH, Gutkind JS. Accelerated wound healing by mTOR activation in genetically defined mouse models. PLoS One. 2010; 5: e10643.
11. Ma D, Lim T, Xu J, Tang H, Wan Y, Zhao H, et al. Xenon preconditioning protects against renal ischemic-reperfusion injury via HIF-1alpha activation. J Am Soc Nephrol. 2009; 20: 713–20.
12. Zhao H, Watts HR, Chong M, Huang H, Tralau-Stewart C, Maxwell PH, et al. Xenon treatment protects against cold ischemia associated delayed graft function and prolongs graft survival in rats. Am J Transplant. 2013; 13: 2006–18.
13. Botusan IR, Sunkari VG, Savu O, Catrina AI, Grünler J, Lindberg S, et al. Stabilization of HIF-1alpha is critical to improve wound healing in diabetic mice. Proc Natl Acad Sci U S A. 2008; 105: 19426–31.
14. Thangarajah H, Vial IN, Grogan RH, Yao D, Shi Y, Januszyk M, et al. HIF-1alpha dysfunction in diabetes. Cell Cycle. 2010; 9: 75–9.
15. Costa PZ, Soares R. Neovascularization in diabetes and its complications. Unraveling the angiogenic paradox. Life Sci. 2013; 92: 1037–45.
16. Martin A, Komada MR, Sane DC. Abnormal angiogenesis in diabetes mellitus. Med Res Rev. 2003; 23: 117–45.
17. Zhuang L, Yang T, Zhao H, Fidalgo AR, Vizcaychipi MP, Sanders RD, et al. The protective profile of argon, helium, and xenon in a model of neonatal asphyxia in rats. Crit Care Med. 2012; 40: 1724–30.
18. Ma D, Hossain M, Chow A, Arshad M, Battson RM, Sanders RD, et al. Xenon and hypothermia combine to provide neuroprotection from neonatal asphyxia. Ann Neurol. 2005; 58: 182–93.
19. Preckel B, Weber NC, Sanders RD, Maze M, Schlack W. Molecular mechanisms transducing the anesthetic, analgesic, and organ-protective actions of xenon. Anesthesiology. 2006; 105: 187–97.
20. Yarin YM, Amarjargal N, Fuchs J, Haupt H, Mazurek B, Morozova S V, et al. Argon protects hypoxia-, cisplatin- and gentamycin-exposed hair cells in the newborn rat's organ of Corti. Hear Res. 2005; 201: 1–9.
21. Loetscher PD, Rossaint J, Rossaint R, Weis J, Fries M, Fahlenkamp A, et al. Argon: neuroprotection in in vitro models of cerebral ischemia and traumatic brain injury. Crit Care. 2009; 13: R206.
22. Jawad N, Rizvi M, Gu J, Adeyi O, Tao G, Maze M, et al. Neuroprotection (and lack of neuroprotection) afforded by a series of noble gases in an in vitro model of neuronal injury. Neurosci Lett. 2009; 460: 232–6.
23. Ma D, Hossain M, Pettet GKJ, Luo Y, Lim T, Akimov S, et al. Xenon preconditioning reduces brain damage from neonatal asphyxia in rats. J Cereb Blood Flow Metab. 2006; 26: 199–208.
24. Mayer B, Soppert J, Kraemer S, Schemmel S, Beckers C, Bleilevens C, et al. Argon Induces Protective Effects in Cardiomyocytes during the Second Window of Preconditioning. Int J Mol Sci. 2016; 17: 1159.
25. Ryang Y-M, Fahlenkamp A V, Rossaint R, Wesp D, Loetscher PD, Beyer C, et al. Neuroprotective effects of argon in an in vivo model of transient middle cerebral artery occlusion in rats. Crit Care Med. 2011; 39: 1448–53.
26. Ulbrich F, Kaufmann KB, Coburn M, Lagrèze WA, Roesslein M, Biermann J, et al. Neuroprotective effects of Argon are mediated via an ERK-1/2 dependent regulation of heme-oxygenase-1 in retinal ganglion cells. J Neurochem. 2015; 134: 717–27.
27. Zhao H, Mitchell S, Koumpa S, Cui YT, Lian Q, Hagberg H, et al. Heme Oxygenase-1 Mediates Neuroprotection Conferred by Argon in Combination with Hypothermia in Neonatal Hypoxia-Ischemia Brain Injury. Anesthesiology. 2016; 125: 180–92.
28. Höllig A, Weinandy A, Liu J, Clusmann H, Rossaint R, Coburn M. Beneficial Properties of Argon After Experimental Subarachnoid Hemorrhage: Early Treatment Reduces Mortality and Influences Hippocampal Protein Expression. Crit Care Med. 2016; 44: e520-9.
29. Okizaki S, Ito Y, Hosono K, Oba K, Ohkubo H, Amano H, et al. Suppressed recruitment of alternatively activated macrophages reduces TGF-β1 and impairs wound healing in streptozotocin-induced diabetic mice. Biomed Pharmacother. 2015; 70: 317–25.
30. Mirza RE, Fang MM, Ennis WJ, Koh TJ. Blocking interleukin-1β induces a healing-associated wound macrophage phenotype and improves healing in type 2 diabetes. Diabetes. 2013; 62: 2579–87.
31. Galiano RD, Tepper OM, Pelo CR, Bhatt KA, Callaghan M, Bastidas N, et al. Topical vascular endothelial growth factor accelerates diabetic wound healing through increased angiogenesis and by mobilizing and recruiting bone marrow-derived cells. Am J Pathol. 2004; 164: 1935–47.

32. Kusumanto YH, van Weel V, Mulder NH, Smit AJ, van den Dungen JJAM, Hooymans JMM, et al. Treatment with intramuscular vascular endothelial growth factor gene compared with placebo for patients with diabetes mellitus and critical limb ischemia: a double-blind randomized trial. Hum Gene Ther. 2006; 17: 683–91.
33. Wieman TJ, Smiell JM, Su Y. Efficacy and safety of a topical gel formulation of recombinant human platelet-derived growth factor-BB (becaplermin) in patients with chronic neuropathic diabetic ulcers. A phase III randomized placebo-controlled double-blind study. Diabetes Care. 1998; 21: 822–7.
34. Kalghatgi S, Friedman G, Fridman A, Clyne AM. Endothelial Cell Proliferation is Enhanced by Low Dose Non-Thermal Plasma Through Fibroblast Growth Factor-2 Release. Ann Biomed Eng. 2010; 38: 748–57.
35. Barton A, Wende K, Bundscherer L, Hasse S, Schmidt A, Bekeschus S, et al. Nonthermal Plasma Increases Expression of Wound Healing Related Genes in a Keratinocyte Cell Line. Plasma Med. 2013; 3: 125–36.
36. Nasruddin, Nakajima Y, Mukai K, Rahayu HSE, Nur M, Ishijima T, et al. Cold plasma on full-thickness cutaneous wound accelerates healing through promoting inflammation, re-epithelialization and wound contraction. Clin Plasma Med. 2014; 2: 28–35.
37. Brun P, Pathak S, Castagliuolo I, Palù G, Brun P, Zuin M, et al. Helium Generated Cold Plasma Finely Regulates Activation of Human Fibroblast-Like Primary Cells. PLoS One. 2014; 9: e104397.
38. Fathollah S, Mirpour S, Mansouri P, Dehpour AR, Ghoranneviss M, Rahimi N, et al. Investigation on the effects of the atmospheric pressure plasma on wound healing in diabetic rats. Sci Rep. 2016; 6: 19144.
39. Cheng K-Y, Lin Z-H, Cheng Y-P, Chiu H-Y, Yeh N-L, Wu T-K, et al. Wound Healing in Streptozotocin-Induced Diabetic Rats Using Atmospheric-Pressure Argon Plasma Jet. Sci Rep. 2018; 8: 12214.
40. Isbary G, Morfill G, Schmidt HU, Georgi M, Ramrath K, Heinlin J, et al. A first prospective randomized controlled trial to decrease bacterial load using cold atmospheric argon plasma on chronic wounds in patients. Br J Dermatol. 2010; 163: no-no.
41. Isbary G, Heinlin J, Shimizu T, Zimmermann JL, Morfill G, Schmidt H-U, et al. Successful and safe use of 2 min cold atmospheric argon plasma in chronic wounds: results of a randomized controlled trial. Br J Dermatol. 2012; 167: 404–10.
42. Brehmer F, Haenssle HA, Daeschlein G, Ahmed R, Pfeiffer S, Görlitz A, et al. Alleviation of chronic venous leg ulcers with a hand-held dielectric barrier discharge plasma generator (PlasmaDerm ® VU-2010): results of a monocentric, two-armed, open, prospective, randomized and controlled trial (NCT01415622). J Eur Acad Dermatology Venereol. 2015; 29: 148–55.
43. Haertel B, von Woedtke T, Weltmann K-D, Lindequist U. Non-thermal atmospheric-pressure plasma possible application in wound healing. Biomol Ther (Seoul). 2014; 22: 477–90.
44. Weltmann K-D, von Woedtke T. Plasma medicine—current state of research and medical application. Plasma Phys Control Fusion. 2017; 59: 014031.
45. Haertel B, Hähnel M, Blackert S, Wende K, von Woedtke T, Lindequist U. Surface molecules on HaCaT keratinocytes after interaction with non-thermal atmospheric pressure plasma. Cell Biol Int. 2012; 36: 1217–22.
46. Duval A, Marinov I, Bousquet G, Gapihan G, Starikovskaia SM, Rousseau A, et al. Cell Death Induced on Cell Cultures and Nude Mouse Skin by Non-Thermal, Nanosecond-Pulsed Generated Plasma. PLoS One. 2013; 8: e83001.
47. Altavilla D, Saitta A, Cucinotta D, Galeano M, Deodato B, Colonna M, et al. Inhibition of lipid peroxidation restores impaired vascular endothelial growth factor expression and stimulates wound healing and angiogenesis in the genetically diabetic mouse. Diabetes. 2001; 50: 667–74.
48. Jia P, Teng J, Zou J, Fang Y, Jiang S, Yu X, et al. Intermittent exposure to xenon protects against gentamicin-induced nephrotoxicity. PLoS One. 2013; 8: e64329.
49. Jeansson M, Gawlik A, Anderson G, Li C, Kerjaschki D, Henkelman M, et al. Angiopoietin-1 is essential in mouse vasculature during development and in response to injury. J Clin Invest. 2011; 121: 2278–89.
50. Bitto A, Minutoli L, Galeano MR, Altavilla D, Polito F, Fiumara T, et al. Angiopoietin-1 gene transfer improves impaired wound healing in genetically diabetic mice without increasing VEGF expression. Clin Sci (Lond). 2008; 114: 707–18.
51. Xiao Y, Reis LA, Feric N, Knee EJ, Gu J, Cao S, et al. Diabetic wound regeneration using peptide-modified hydrogels to target re-epithelialization. Proc Natl Acad Sci U S A. 2016; 113: E5792–801.
52. Balaji S, Han N, Moles C, Shaaban AF, Bollyky PL, Crombleholme TM, et al. Angiopoietin-1 improves endothelial progenitor cell-dependent neovascularization in diabetic wounds. Surgery. 2015; 158: 846–56.
53. Mendoza-Naranjo A, Cormie P, Serrano AE, Wang CM, Thrasivoulou C, Sutcliffe JES, et al. Overexpression of the gap junction protein Cx43 as found in diabetic foot ulcers can retard fibroblast migration. Cell Biol Int. 2012; 36: 661–7.
54. Xuan YH, Huang B Bin, Tian HS, Chi LS, Duan YM, Wang X, et al. High-glucose inhibits human fibroblast cell migration in wound healing via repression of bFGF-regulating JNK phosphorylation. PLoS One. 2014; 9: e108182.
55. Al-Mulla F, Leibovich SJ, Francis IM, Bitar MS. Impaired TGF-β signaling and a defect in resolution of inflammation contribute to delayed wound healing in a female rat model of type 2 diabetes. Mol Biosyst. 2011; 7: 3006–20.
56. Khanna S, Biswas S, Shang Y, Collard E, Azad A, Kauh C, et al. Macrophage Dysfunction Impairs Resolution of Inflammation in the Wounds of Diabetic Mice. PLoS One. 2010; 5: e9539.
57. Mirza R, Koh TJ. Dysregulation of monocyte/macrophage phenotype in wounds of diabetic mice. Cytokine. 2011; 56: 256–64.
58. Miao M, Niu Y, Xie T, Yuan B, Qing C, Lu S. Diabetes-impaired wound healing and altered macrophage activation: a possible pathophysiologic correlation. Wound Repair Regen. 2012; 20: 203–13.
59. Jetten N, Roumans N, Gijbels MJ, Romano A, Post MJ, de Winther MPJ, et al. Wound administration of M2-polarized macrophages does not improve murine cutaneous healing responses. PLoS One. 2014; 9: e102994.
60. Grochot-Przeczek A, Lach R, Mis J, Skrzypek K, Gozdecka M, Sroczynska P, et al. Heme Oxygenase-1 Accelerates Cutaneous Wound Healing in Mice. PLoS One. 2009; 4: e5803.
61. Jazwa A, Loboda A, Golda S, Cisowski J, Szelag M, Zagorska A, et al. Effect of heme and heme oxygenase-1 on vascular endothelial growth factor synthesis and angiogenic potency of human keratinocytes. Free Radic Biol Med. 2006; 40: 1250–63.
62. Shu Y, Patel SM, Pac-Soo C, Fidalgo AR, Wan Y, Maze M, et al. Xenon pretreatment attenuates anesthetic-induced apoptosis in the developing brain in comparison with nitrous oxide and hypoxia. Anesthesiology. 2010; 113: 360–8.
63. Jia P, Teng J, Zou J, Fang Y, Wu X, Liang M, et al. Xenon Protects Against Septic Acute Kidney Injury via miR-21 Target Signaling Pathway. Crit Care Med. 2015; 43: e250-9.
64. Al-Mashat HA, Kandru S, Liu R, Behl Y, Desta T, Graves DT. Diabetes enhances mRNA levels of proapoptotic genes and caspase activity, which contribute to impaired healing. Diabetes. 2006; 55: 487–95.